A Digital Implementation of Continuous-time Ripple Correlation Control for Photovoltaic Applications

Kevin P. Kroeger, Sanghun Choi, Ali M. Bazzi, Brian B. Johnson, and Philip T. Krein
Grainger Center for Electric Machinery and Electromechanics
Department of Electrical and Computer Engineering
University of Illinois at Urbana-Champaign
1406 W. Green St. Urbana, IL 61801 USA

***Abstract* — A new digital implementation of continuous-time ripple correlation control (RCC) for maximum power point tracking of photovoltaic (PV) panels. This implementation is straightforward and provides easy and convenient expansion to multiple-panel PV systems. The simple graphical user interface developed helps control and monitor the panels, with the options of manual control or RCC. Digital implementation provides a suitable environment for phase-shift compensation which usually leads to convergence problems with RCC. Results show that over 95% convergence accuracy is achieved using the proposed implementation.**

***Index Terms* — Maximum power point tracking, ripple correlation control, digital control of photovoltaics, multi-panel phovoltaic systems, microconverter**

I. Introduction

Maximum power point tracking (MPPT) for PVs is the process by which the maximum available power is drawn from a system despite variable weather conditions. There are many different ways to implement MPPT; the most common are perturb and observe, fractional open circuit voltage, incremental conductance, and hill climbing. These and several others are compared in detail in [1]. Most of these methods have applications with analog and digital implementations with each having its own advantages.

Ripple correlation control (RCC) [2,3] has been verified to be extremely fast, accurate, and simple. It is a dynamic optimization technique that uses ripple present in any switching power converter to drive a cost function, such as the power of a PV panel, to a local optimum. In an MPPT application with a boost converter at the panel terminals, the fundamental control law for RCC can be simplified into (1) where I_L is the inductor current and I_L^* is the inductor current at the maximum power point.

$$\begin{aligned} I_L < I_L^* \Rightarrow \frac{dp}{di_L} > 0 \Rightarrow \frac{di_L}{dt}\frac{dp}{dt} > 0 \\ I_L > I_L^* \Rightarrow \frac{dp}{di_L} < 0 \Rightarrow \frac{di_L}{dt}\frac{dp}{dt} < 0 \end{aligned} \quad (1)$$

RCC is parameter insensitive and asymptotically converges to the true maximum power point of a PV panel provided there is only one local maximum [2]. Convergence speed is limited only by switching frequency and controller gain.

Multiple implementations of the RCC control law are discussed in [2,3]. As the purpose of RCC is to control a switching power converter, the ideal controller output would be a duty ratio or switching signal. Combining that with the RCC control law (1), integral control shown in (2) is appropriate.

$$d = k \int \frac{di_L}{dt}\frac{dp}{dt} dt \quad (2)$$

In (2), k is the integral control gain and has effects on stability and convergence speed, as demonstrated in [2]. The derivatives of current and power can be approximated by high-pass filters [4] so long as the cutoff frequency is set above the ripple frequency. The cutoff frequencies of the two filters must also be the same to avoid introducing relative phase shifts between the two ripples.

A different approach from that shown in [2, 3] is to formulate RCC [5]. In [5] the analog formulation in (2) is adapted and changed to a discrete implementation that compares the power at two different points within a single switching cycle and adjusts the duty ratio accordingly. This is different from a perturb and observe method because the controller does not wait for the system to reach steady state. The approach does not implement the control laws presented and implemented in [2] and instead uses its own separately derived control laws. The key issue is determining when to sample the waveform to obtain useful data. Determining the maximum power point is further complicated by array capacitance and other effects.

PV panel capacitance can be modeled as a capacitor in parallel with the PV panel [6]. It introduces a phase shift in the inductor current relative to the true PV current. The phase shift causes RCC, under current correlation, to shift slightly from the true maximum power point. One method to counteract the capacitive phase shift is to use voltage and power correlation instead of current and power correlation [2, 5]. Current correlation can still be used if additional steps are taken to mitigate the capacitance effects. Implementing and tuning a phase compensator could be tedious in analog circuitry, but it is simple to build digitally using basic control theory [7].

978-1-4244-5901-8/10/$26.00 ©2010 IEEE

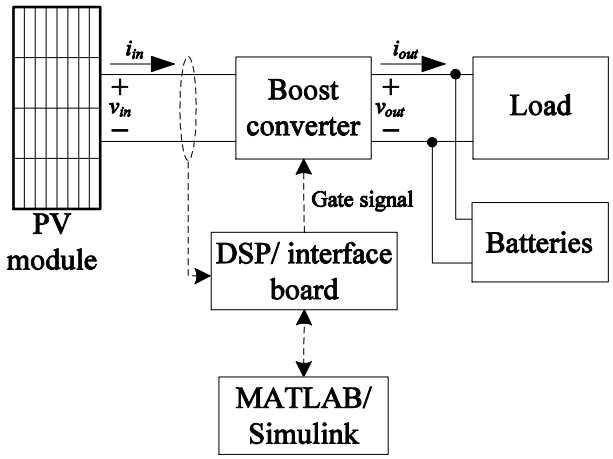

Fig. 1. Overview of the proposed system configuration.

Such a compensator can be designed to produce a fixed phase offset that can be tuned to provide optimum power over a broad range of operating conditions.

An implementation of RCC applied to MPPT with built-in monitoring capabilities and a central management system that can be easily expanded to multiple panels has not yet been documented. Also, the digital implementation of continuous-time RCC laws has not been shown. Additionally, adding a compensator under such a scenario would be a major advantage. In this paper, we introduce the digital implementation of continuous-time RCC on a digital signal processor (DSP) with several advantages including a compensator for panel capacitance effects, real-time control and monitoring, and ease of expansion to multiple panels. Section II presents the proposed system. Section III describes the experimental setup and Section IV presents experimental results. Section V concludes with remarks and future work.

II. Proposed System

A single-panel system is studied under RCC control and real-time monitoring implemented on a DSP, as shown in Fig. 1. A PV module is connected through a power converter to supply power to a load. The DSP/interface board receives voltage and current information directly from the PV panel outputs. The DSP takes the information from the interface board and executes RCC with all required information being available to the operator through a friendly graphical user interface (GUI). In Fig. 1, i_{in} is the panel current, v_{in} is thepanel voltage, i_{out} is the load current, v_{out} is the load voltage, and the gate signal controls the boost converter.

A phase compensator is needed to mitigate the errors associated with panel capacitance. The lead compensator was

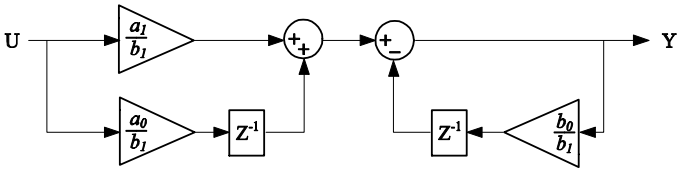

Fig. 2. Block diagram of discrete-time lead compensator.

implemented in Simulink to cancel the negative phase shift between the inductor current and the PV current. The transfer function of the lead compensator (3) and the constant α (4) were studied in [7]. If ω_c is the chosen corner frequency of the high-pass filter, then $T = \frac{1}{\omega_c}$, and φ_{max} is the maximum phase shift. Note that this transfer function is completely specified for chosen ω_c and φ_{max}.

$$G_c(s) = \sqrt{\alpha}\,\frac{Ts+1}{\alpha Ts+1} \tag{3}$$

$$\alpha = \frac{1-\sin\phi_{max}}{1+\sin\phi_{max}} \tag{4}$$

This transfer function is only applicable to analog systems. In order to implement the transfer function on the DSP, it must first be discretized into the general form shown in (5), where Y and U are the output and input signals, respectively. Equation (5) can be rewritten as (6) through simple algebra, and represented as the block diagram in Fig. 2.

$$G_c(z) = \frac{Y}{U} = \frac{a_1 z + a_0}{b_1 z + b_0} = \frac{a_1 + a_0 z^{-1}}{b_1 + b_0 z^{-1}} \tag{5}$$

$$Y = \frac{(a_1 + a_0 z^{-1})U - b_0 Y z^{-1}}{b_1} \tag{6}$$

The lead compensator has a frequency-dependent phase response such that only the chosen center frequency, ω_c, is shifted by the maximum amount, φ_{max}, as shown in Fig. 3. Given that the inductor time constant is much greater than the switching period, the current ripple waveform is roughly triangular. The lead compensator was designed with a center frequency of 10kHz so that the fundamental component of the ripple waveform was shifted by φ_{max}. and was sampled at an interval of T_s. For the single panel implementation T_s was set to 10μs to give 10 samples per period.

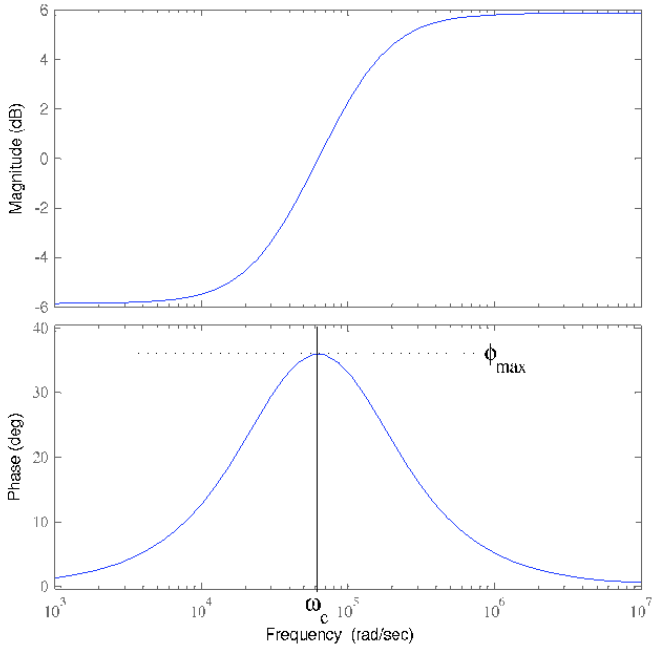

Fig. 3. Magnitude and phase response of lead compensator

As shown in Fig. 4, the lead compensator shifts the entire waveform by the amount determined by the user for a sine wave input. As high-pass filters are used to extract the ripple, the derivative waveforms look sinusoidal at 10kHz, even though they are exponential and close to triangular. This method of extraction helps mitigate the harmonic effects present in a triangular waveform.

Discrete-time RCC was implemented in Simulink. The control law in (2) was discretized to function on the DSP. The ripple correlator takes the derivative or ripple information of the power and current and uses a discrete time integrator. This expression outputs a duty ratio as seen in (7).

$$d = k\tilde{P}\tilde{I}\frac{T_S}{z-1} \qquad (7)$$

$\tilde{P}$ and $\tilde{I}$ represent the ripples of power and current respectively which are supplied by identical high-pass filters.

Such an implementation of RCC is very flexible and maintains simplicity. Because of the lead compensator, the process can be adapted to any configuration. This increases the range of applications of the design. Even though this implementation uses only a single PV panel, an array of several panels, up to 6 panels in this system, could be used with only the single central controller, eliminating the need for populating, debugging, and maintaining multiple control boards. Further, the centralized control board allows easy implementation of a GUI for control and monitoring. Previous implementations of RCC have been single-panel test beds, however, this digital implementation lends itself to multiple panel testing.

III. Experimental Setup

The MPPT and monitoring algorithms were employed on an eZdspF2812. The DSP is programmed using MATLAB Simulink in conjunction with the Real Time Data Exchange and Code Composer Studio. The ezdspf2812 includes the TMS320F2812 DSP and has 16 analog-to-digital converters and 6 dual PWM channels. For just a single panel application

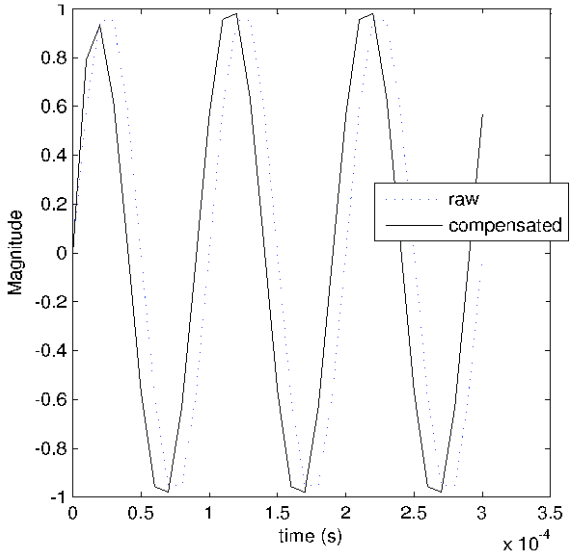

Fig. 4. Effects of lead compensator on sine wave

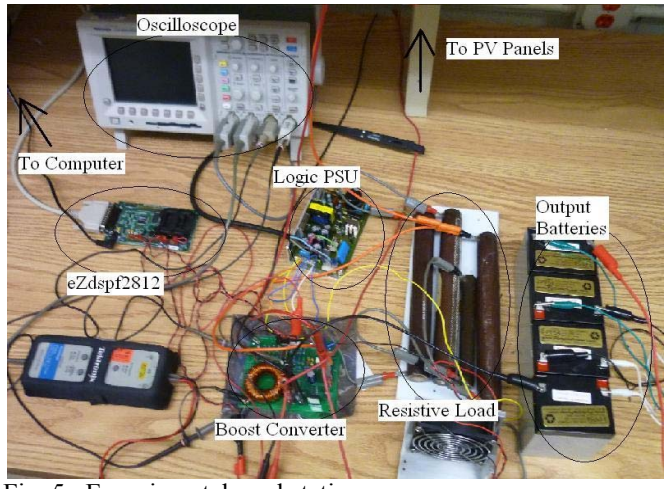

Fig. 5. Experimental workstation

a less powerful DSP or even a cheap analog circuit could be used, but the main advantage of this implementation is its expansion flexibility.

The hardware includes a microconverter for each PV panel in an array. To ensure functionality over a wide range of operating conditions, a boost converter was chosen and built using components shown in table 1.

TABLE I
BOOST CONVERTER COMPONENTS

Component	MOSFET	DIODE	Current Sensors	Inductor
Specifications	IRFPS3815	MBR10100	ACS712	2mH

To increase compatibility with the DSP, an interface board was built. [2] demonstrates the effect of increased switching frequency on RCC convergence; based on this, a switching frequency of 10kHz was chosen to balance convergence requirements and component size. The experimental setup is shown in Fig. 5.

The graphical user interface was designed in Simulink. Fig. 6 shows an example of the GUI for a single panel. From top to

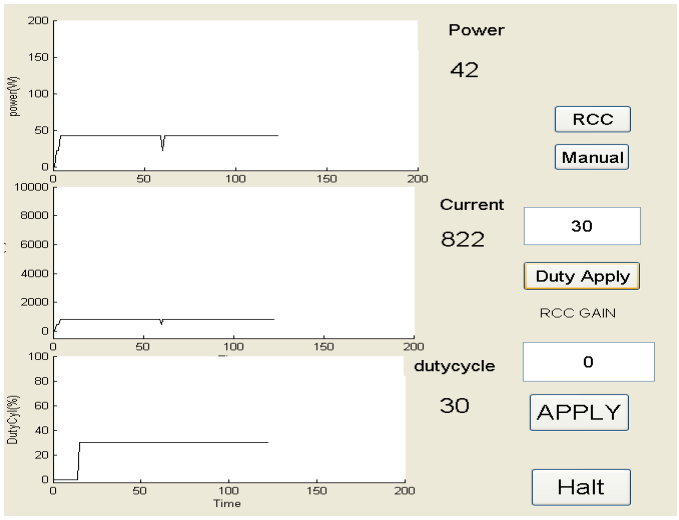

Fig. 6. Single panel GUI

bottom are power (W), current (mA), and converter duty ratio (%). The waveforms are averaged and then shown on a large time scale of 0-200s so that the progression of the duty ratio and power as the RCC converges can be observed.

IV. Experimental Results

Performance was verified experimentally using a BP Solar model #BP7185N mounted at a fixed 50° angle on a mid November day. The maximum output power (P_{max}), open-circuit voltage (V_{oc}), and short-circuit current (I_{sc}) are shown in Table 2. The PV panel was connected through a long (>15m) wire to the boost circuit and control. The load tested was a 26.2Ω resistance in parallel with four 12V sealed lead acid batteries for a combined 48V output. The added batteries on the output fixed the output voltage at approximately 48V. When the PV panel was supplying more power than could be dissipated in the resistors, the excess power was stored in the battery bank. Likewise, in cloudy, rainy, or dark conditions the batteries could supply the necessary excess power to the resistors to maintain the voltage level at 48V. Note that the fixed output voltage does not interfere with the converter operation or the RCC convergence as the inductor current still varies directly with the duty ratio.

Data was taken to ensure proper RCC phase relationships using open-loop duty-ratio control, also implemented on the DSP. Figures 7 and 8 show, in order from top to bottom: voltage (20V/div), power (50W/div), current (1A/div), and the boost converter switching signal (5V/div). The waveforms are shown on a 100µs/div time scale. In Fig. 7 the duty ratio is set below the optimum, causing $I_L < I_L^*$ and the current and power to be in phase. This satisfies the first condition of (1). Fig. 8 shows the effects of the duty ratio set higher than the optimum, causing $I_L > I_L^*$ and the current and power to be 180° out of phase. This is also consistent with (1). The closed loop control was tested with the compensator on the current measurement, and the initial duty ratio set at zero. In this state the PV panel sees an open circuit. At an arbitrary time, RCC is enabled and the duty ratio climbs from zero to the steady state duty ratio corresponding to the true maximum power point.

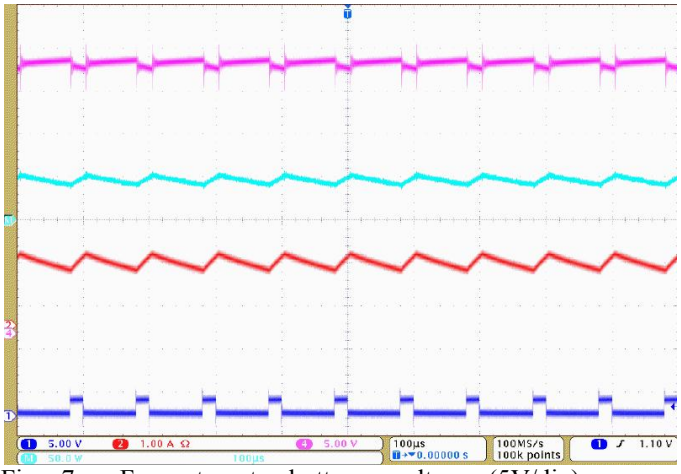

Fig. 7. From top to bottom: voltage (5V/div), power (50W/div), current (1A/div), and gating signal (5V/div) on a 100µs time scale for the case where $I_L < I_L^*$

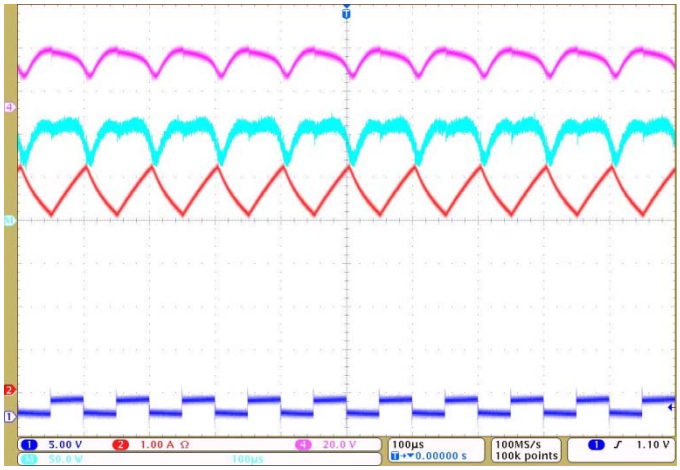

Fig. 8. From top to bottom: voltage (5V/div), power (50W/div), current (1A/div), and gating signal (5V/div) on a 100µs time scale for the case where $I_L > I_L^*$

The true optimum was determined via open-loop control to be at a duty cycle of 37% while RCC converged to 35%, as shown in Fig. 9. Clearly, the power has significantly increased in Fig. 9, as compared to Figures 7 and 8. Fig. 7 shows an average power of ~50W while in Fig. 8 the average power is ~90W, compared to ~140W in Fig. 9. The compensator improved the maximum power tracking from 90% of the true optimum to over 95%.

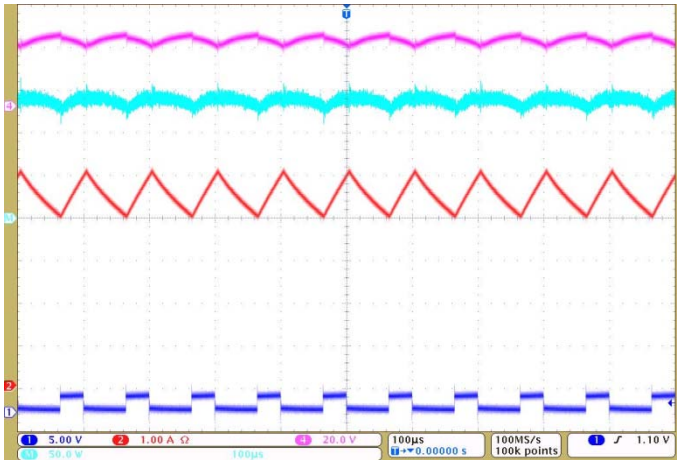

Fig. 9. From top to bottom: voltage (5V/div), power (50W/div), current (1A/div), and gating signal (5V/div) on a 100µs time scale for the case where $I_L \approx I_L^*$

V. Conclusion and Future Work

A digital implementation of ripple correlation control based on a continuous-time analog formulation was presented. The performance of the method was examined in experiments. The results showed the addition of a lead compensator to account for the impact of panel capacitance and wire inductance. This simple digital implementation is user friendly and allows for use of centralized control and monitoring of multiple MPPTs in multi-panel installations. Such a scenario with multiple panels is currently under development where the convergence speed, central management and monitoring, and different series-parallel combinations of the panels will be studied.

ACKNOWLEDGMENT

This research is supported by the Grainger Center for Electric Machinery and Electromechanics.

REFERENCES

[1] Esram, T.; Chapman, P.L., "Comparison of Photovoltaic Array Maximum Power Point Tracking Techniques," *IEEE Transactions on Energy Conversion,* , vol.22, no.2, pp.439-449, June 2007.

[2] Esram, T.; Kimball, J.W.; Krein, P.T.; Chapman, P.L.; Midya, P., "Dynamic Maximum Power Point Tracking of Photovoltaic Arrays Using Ripple Correlation Control," *, IEEE Transactions on Power Electronics* , vol.21, no.5, pp.1282-1291, Sept. 2006.

[3] Krein, P.T., "Ripple correlation control, with some applications," *IEEE International Symposium on Circuits and Systems, 1999*, vol.5, pp.283-286.

[4] Logue, D.L.; Krein, P.T., "Observer-based techniques in ripple correlation control applied to power electronic systems," *IEEE Power Electronics Specialists Conference, 2001*, vol.4, no., pp.2014-2018, 2001 .

[5] Kimball, J.W.; Krein, P.T., "Discrete-Time Ripple Correlation Control for Maximum Power Point Tracking," *IEEE Transactions on Power Electronics,* , vol.23, no.5, pp.2353-2362, Sept. 2008.

[6] Brambilla, A.; Gambarara, M.; Garutti, A.; Ronchi, F., "New approach to photovoltaic arrays maximum power point tracking ," *IEEE Power Electronics Specialists Conference, 1999*, vol.2, no., pp.632-637, 1999.

[7] Ogata, Katsuhiko. *Modern Control Engineering,* 4th ed. Englewood Cliff, NJ: Prentice-Hall, Inc. 1970.